

The Metalloprotease ADAMTS8 Displays Antitumor Properties through Antagonizing EGFR–MEK–ERK Signaling and Is Silenced in Carcinomas by CpG Methylation

Gigi C.G. Choi¹, Jisheng Li^{1,2}, Yajun Wang¹, Lili Li¹, Lan Zhong¹, Brigitte Ma¹, Xianwei Su¹, Jianming Ying^{1,3}, Tingxiu Xiang⁴, Sun Young Rha⁵, Jun Yu⁶, Joseph J.Y. Sung⁶, Sai Wah Tsao⁷, Anthony T.C. Chan¹, and Qian Tao¹

Abstract

A disintegrins and metalloproteinases with thrombospondin motifs (ADAMTS) family members have been reported dysregulated in various cancers. Through refining a loss of heterozygosity locus at 11q25 by array-CGH, we identified *ADAMTS8* as a novel candidate tumor suppressor gene. Although *ADAMTS8* downregulation has been reported in several tumors, its biologic function and underlying mechanism remain largely unknown. Here, we found that *ADAMTS8* is broadly expressed in normal tissues but frequently downregulated or silenced by promoter methylation in common carcinoma cell lines, including nasopharyngeal, esophageal squamous cell, gastric, and colorectal carcinomas. Pharmacologic or genetic demethylation restored *ADAMTS8* expression, indicating that promoter methylation mediates its silencing. Aberrant methylation of *ADAMTS8* was also detected in several types of primary tumors but rarely in normal tissues. Further functional studies showed that restoring *ADAMTS8* expression suppressed tumor cell clonogenicity through inducing apoptosis. *ADAMTS8* as a secreted protease inhibited epidermal growth factor receptor (EGFR) signaling along with decreased levels of phosphorylated MEK and ERK. We further found that *ADAMTS8* disrupted actin stress fiber organization and inhibited tumor cell motility. Thus, our data demonstrate that *ADAMTS8* metalloprotease acts as a functional tumor suppressor through antagonizing EGFR–MEK–ERK signaling, in addition to its previously reported anti-angiogenesis function, and is frequently methylated in common tumors.

Implications: This study uncovers the tumor suppressive function of *ADAMTS8*, one of the ADAMTS family members, and its frequent methylation in certain tumors could be developed as a potential biomarker. *Mol Cancer Res*; 12(2); 228–38. ©2013 AACR.

Introduction

Metalloproteinases are initially regarded to facilitate tumor progression by promoting angiogenesis and metastatic dissemination of cancer cells through extracellular matrix

(ECM) degradation (1). However, this concept is challenged by recent findings of several members showing to possess tumor suppressive functions (2–6). A disintegrins and metalloproteinases with thrombospondin motifs (ADAMTS), a family of extracellular metalloproteases, is structurally and functionally similar to matrix metalloproteinases (MMP) and ADAMs (7). Unlike ADAMs mainly as trans-membrane proteins, ADAMTSs are secreted proteinases binding to ECM (8). Dysregulated expression of ADAMTSs, such as *ADAMTS1* (2), *ADAMTS8*, *ADAMTS9* (5), *ADAMTS12* (3), *ADAMTS15* (4), *ADAMTS18* (6), and *ADAMTS20* (9, 10), have been detected in diverse types of malignancies including lung, brain, breast, gastric, prostate, pancreatic cancers, and glioblastoma (8). Various ADAMTSs have been shown to regulate cell proliferation, adhesion, migration, angiogenesis, and intracellular signaling (8, 11), thus involved in multiple tumor pathogenesis (1, 6).

ADAMTS8 is 1 of the 3 ADAMTS members with anti-angiogenic property, indicating its potential as a tumor suppressor (5, 12, 13). Downregulation of *ADAMTS8* has been found in some tumors, such as brain tumors (14), breast carcinoma (9), non-small cell lung carcinoma (15), head and neck squamous cell carcinoma (16), and pancreatic

Authors' Affiliations: ¹Cancer Epigenetics Laboratory, Department of Clinical Oncology, State Key Laboratory of Oncology in South China, Sir YK Pao Center for Cancer and Li Ka Shing Institute of Health Sciences, The Chinese University of Hong Kong, Hong Kong; ²Department of Chemotherapy, Cancer Center, Qilu Hospital, Shandong University, Jinan, Shandong, China; ³Department of Pathology, Cancer Hospital, Peking Union Medical College & Chinese Academy of Medical Sciences, Beijing, China; ⁴The First Affiliated Hospital of Chongqing Medical University, Chongqing, China; ⁵Department of Internal Medicine, Yonsei University College of Medicine, Korea; ⁶State Key Laboratory of Digestive Diseases, Department of Medicine and Therapeutics, The Chinese University of Hong Kong; ⁷Departments of Anatomy, University of Hong Kong, Hong Kong

Note: Supplementary data for this article are available at Molecular Cancer Research Online (<http://mcr.aacrjournals.org/>).

G.C.G. Choi, J. Li, and Y. Wang contributed equally to this work.

Corresponding Author: Qian Tao, Room 315, Cancer Center, PWH, The Chinese University of Hong Kong, Shatin, Hong Kong. Phone: 852-2632-1340; Fax: 852-2648-8842; E-mail: qtiao@clo.cuhk.edu.hk

doi: 10.1158/1541-7786.MCR-13-0195

©2013 American Association for Cancer Research.

cancer (17), whereas its expression in other common solid tumors including nasopharyngeal (NPC), esophageal squamous cell (ESCC), gastric, colorectal (CRC), renal (RCC), and cervical carcinomas remains unclear.

Genetic and epigenetic alterations especially promoter methylation and histone modifications play a crucial role in tumor initiation and progression, although leading to activation of oncogene and inactivation of tumor suppressor gene (TSG). Promoter methylation of *ADAMTS8* has been detected in brain tumors (14), non-small cell lung carcinoma (15) and thyroid cancer (18), which also could serve as one of the signatures for primary thyroid cancer (18), suggesting that epigenetic silencing of *ADAMTS8* may be involved in tumorigenesis. However, its tumor suppressive functions and underlying mechanisms in tumor pathogenesis are largely unknown.

Through refining an LOH locus at 11q25 by 1-Mb array comparative genomic hybridization (array-CGH) and expression profiling of the affected genes, we identified *ADAMTS8* as a candidate TSG. In this study, we examined the expression and methylation of *ADAMTS8* in common solid carcinomas and further explored its tumor suppressive functions and relevant mechanisms in tumorigenesis.

Materials and Methods

Cell lines, tumors, and normal tissue samples

Multiple cell lines of NPC, ESCC, gastric, and CRC, hepatocellular (HCC), lung, breast, RCC, and cervical carcinomas and several immortalized normal epithelial cell lines were used (19, 20). Cell lines were obtained either from the American Type Culture Collection or our collaborators. HCT116-DKO cell line with double knockout of DNA methyltransferases DNMT1 and DNMT3B was also used (gifts of Bert Vogelstein, Johns Hopkins University, Baltimore, MD). Cell lines were treated with 10 mmol/L 5-aza-2'-deoxycytidine (Aza; Sigma-Aldrich) for 3 days or further treated with 100 nmol/L trichostatin A (TSA; Cayman Chemical Co.) for additional ~16 hours as described previously (21).

Human normal adult and fetal tissue RNA samples were purchased commercially (Stratagene or Millipore-Chemicon; refs. 20 and 22). Genomic DNA samples of normal nasopharyngeal and gastric tissues, as well as primary tumor tissues of nasopharyngeal carcinoma, gastric cancer, and colorectal carcinoma, have been described previously (19, 23–25). Clinical information was available for the majority of gastric cancer samples.

Semiquantitative reverse transcription-PCR and quantitative real-time RT-PCR

Semiquantitative reverse transcription-PCR (RT-PCR) and quantitative real-time PCR (qPCR) were performed as described previously (21, 26). RT-PCR was performed for 32 cycles using Go-Taq Flexi DNA polymerase (Promega). SYBR Green master mix (Applied Biosystems) was used for real-time PCR analysis. *GAPDH* was used as

an internal control. Primers are listed in Supplementary Table S1.

Methylation-specific PCR and bisulfite genomic sequencing

Bisulfite treatment of genomic DNA, methylation-specific PCR (MSP), and bisulfite genomic sequencing (BGS) were performed as described previously (22, 27). Briefly, 1 μ m of bisulfite-treated DNA (around 50 ng) was used for MSP amplified by using 0.625 U of AmpliTaq Gold polymerase (Applied Biosystems) with 2.0 mmol/L MgCl₂ and 0.2 mmol/L dNTP in a 25 μ L reaction volume. PCR was performed at 95°C for 10 minutes, followed by 40 cycles consisting of 94°C for 30 seconds, annealing at 60°C (methylation detection) or 58°C (unmethylation detection) for 30 seconds, and 72°C for 30 seconds, and a final extension at 72°C for 5 minutes. PCR products were analyzed on a 1.8% agarose gel. For BGS, bisulfite-treated DNA was amplified for using BGS primers, and the PCR products were cloned into the PCR4-TOPO vector (Invitrogen). In all, 6 to 10 colonies were randomly chosen and sequenced. MSP and BGS primers are shown in Supplementary Table S1.

ADAMTS8 deletion analysis

Homozygous deletion of *ADAMTS8* coding exon 1 and exon 2 was examined using multiplex genomic DNA PCR as previously described (20, 23). A 301-bp fragment and a 349-bp fragment of the *ADAMTS8* were amplified along with a 134-bp fragment of *APRT* as internal control. The PCR was performed in a 12.5 μ L reaction mixture consisting of 0.4 μ mol/L of primers located on *ADAMTS8* exon 1 and exon 2, 0.2 μ mol/L of *APRT* primers, 0.2 mmol/L of dNTP, 2.0 mmol/L of MgCl₂, 1 \times PCR Buffer II, 0.3125 U of AmpliTaq Gold (Applied Biosystems), and 50 ng of template DNA. PCR was conducted as 95°C for 10 minutes, then 35 cycles (94°C, 30 seconds; 55°C, 30 seconds; 72°C, 30 seconds), followed by 72°C for 10 minutes. PCR products were analyzed on 1.8% agarose gels. Primers are listed in Supplementary Table S1.

Construction of ADAMTS8-expressing vectors

The full-length open reading frame of *ADAMTS8* was cloned from normal adult larynx cDNA library into pCR4-TOPO vector (Invitrogen). A Flag tag was fused to the C-terminal of ADAMTS8 by PCR amplification and the coding sequence of ADAMTS8-Flag was subcloned into pcDNA3.1(+) with *Bam*HI and *Xho*I to generate pcDNA3.1(+)-ADAMTS8-Flag. ADAMTS8 was further subcloned into the pEGFP-N1 vector to generate a pEGFP-N1-ADAMTS8. All PCR reactions were performed with AccuPrime polymerase (Invitrogen) and all cloned fragments were validated by sequencing.

Immunofluorescence

Cells grown on coverslips were stained by immunofluorescence as described previously (19, 20). In brief, HONE1 or KYSE150 cells were transfected with pcDNA3.1

(+)-ADAMTS8-Flag or pEGFP-N1-ADAMTS8 plasmid. At 48-hour posttransfection, cells were fixed with 4% (w/v) paraformaldehyde before staining with primary and FITC-conjugated secondary antibodies (F313; Dako) for half an hour at 37°C. For actin staining, cells were stained with rhodamine-conjugated phalloidin for 1 hour at 37°C. Cells were counterstained with 4',6-diamidino-2-phenylindole (DAPI) before analysis using Olympus BX51 microscope (Olympus Corporation) and Leica TCS SP5 confocal microscope (Leica Microsystems CMS GmbH).

Colony formation assay

Clonogenicity was determined by measuring colonies growing in monolayer culture as described previously (6, 21). HONE1 and KYSE150 cells (1×10^5 per well) were seeded in a 12-well plate and were transiently transfected with pcDNA3.1(+)-ADAMTS8-Flag plasmid or the pcDNA3.1 vector alone, using FuGENE 6 (Roche). At 48-hours posttransfection, cells were collected and plated at appropriate density in a 6-well plate under G418 (0.4 mg/mL) selection for 2 to 3 weeks. Cell colonies were fixed and stained with Gientian Violet (ICM Pharma) before counting of surviving colonies (>50 cells per colony). Statistical analysis was performed with Student *t* test, $P < 0.05$ was considered as statistically significant difference.

Cell-proliferation assay

MTS (Promega) assay was performed according to the manufacturer's instruction. Cells were seeded in 96-well plates at a density of 1 to 2×10^3 , 15 μ L MTS solution was added into each well at indicated time points and then incubated for 3 hours at 37°C. Effect of cell number on absorbance at 490 nm was measured. The experiments were performed in triplicate and repeated 3 times.

Apoptosis assay

HONE1 and KYSE150 cells were seeded on glass coverslips and fixed in 4% paraformaldehyde. Cells were permeabilized with 0.1% Triton X-100 in PBS for 5 minutes on ice. Apoptotic cells with strand breaks in DNA were stained using the *In Situ* Cell Death Detection Kit, Fluorescein (Roche) according to Manufacturer's protocol. The labeling reaction was performed by incubating each sample with terminal deoxynucleotidyl transferase-mediated dUTP nick end labeling (TUNEL) reaction mixture containing terminal deoxynucleotidyl transferase and fluorescein-labeled dUTP at 37°C for 1 hour. DAPI was used to stain total nuclei. Coverslips were mounted on glass slides and analyzed under a fluorescence microscope. Apoptotic cells with condensed or fragmented nuclei were also examined by DAPI staining.

Western blot analysis

HONE1 and KYSE150 cells were transiently transfected with pcDNA3.1(+)-ADAMTS8-Flag plasmid or the pcDNA3.1 vector alone using FuGENE 6 (Roche). At 48-hour posttransfection, cells were harvested and lysed in lysis buffer [10 mmol/L Tris-HCl (pH 7.4), 1% SDS, 10%

glycerol, 5 mmol/L MgCl₂, 1 mmol/L phenylmethylsulfonyl fluoride, 1 mmol/L sodium orthovanadate, 5 μ g/mL leupeptin, and 21 μ g/mL aprotinin]. Protein samples were incubated for 30 minutes on ice and followed by centrifugation to remove cell debris. Supernatant containing 30 μ g of total protein lysate from each sample was subjected to SDS-PAGE and transferred onto a polyvinylidene difluoride membranes which were probed with anti-MEK1/2, anti-ERK1/2, anti-phospho-MEK1/2 (Ser²¹⁷/Ser²²¹), anti-phospho-ERK1/2 (Thr²⁰²/Tyr²⁰⁴; Cell Signaling Technology); anti-epidermal growth factor receptor (EGFR; BD Transduction Laboratories); anti-phospho-EGFR (Tyr¹⁰⁸⁶; Invitrogen); anti-Flag (Sigma-Aldrich), or anti-tubulin (Lab Vision Corporation) primary antibodies. Protein bands were visualized by enhanced chemiluminescence detection system (GE Healthcare Bio-Sciences).

Conditioned medium

Conditioned medium containing secreted ADAMTS8 was collected from pcDNA3.1(+)-ADAMTS8-Flag-transfected KYSE150 and HONE1 cells cultured in RPMI 1640 with 3% FBS for indicated times after centrifuged at 1,000 g for 30 minutes. KYSE150 cells were treated with conditioned medium containing ADAMTS8 for 24 hours and collected for further study.

Luciferase reporter assay

Reporter activity of the serum response element (SRE)-luc, AP-1 plasmids (Stratagene) was determined in HONE1 and KYSE150 cells as described previously (19, 28). Subconfluent cells in 24-well plates were transiently cotransfected with pSRE-luc, pcDNA3.1(+)-ADAMTS8-Flag and pRL-SV40. After 48 hours, cells were harvested for luciferase activity measurement using Dual-Luciferase Reporter Assay System (Promega). Activity of the firefly luciferase reporter (SRE)-luc and AP-1-luc were normalized with the activity of the renilla luciferase pRL-SV40 as an internal control to correct the differences in transfection efficiency. Each experiment was performed in triplicates and was repeated 3 times.

Wound healing assay

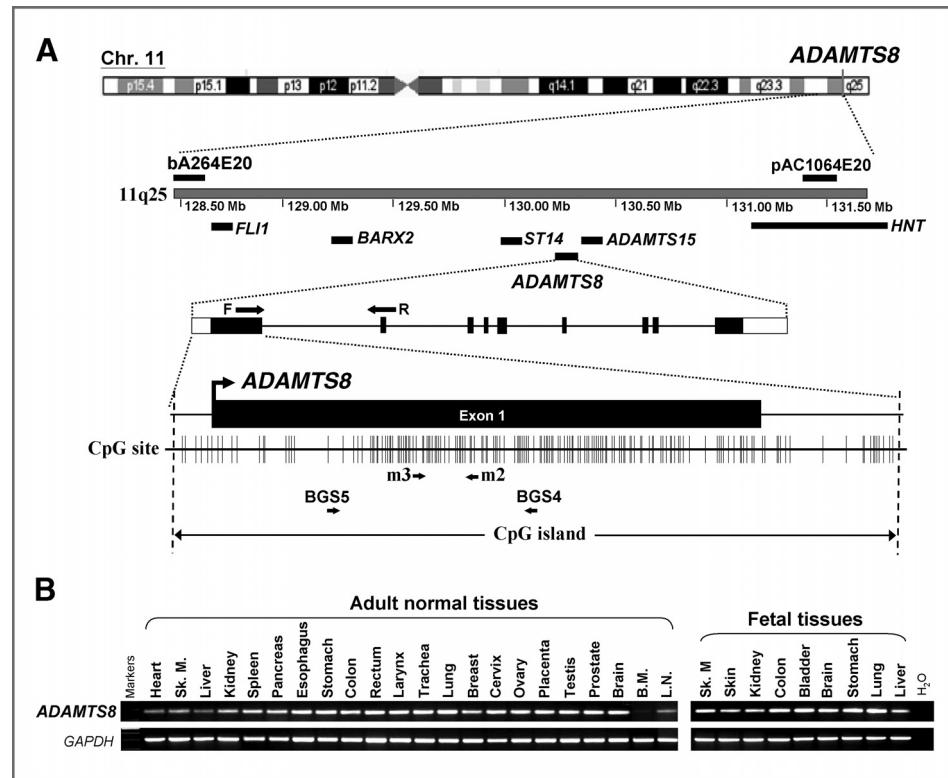
Cell motility of HONE1 and KYSE150 cells transfected with pEGFP-N1-ADAMTS8 or control pEGFP-N1 vector was assessed using a scratch wound assay. Cells were cultured in 6-well dishes until confluent before using sterile tips to scratch a wound. After rinsing with PBS, cells were incubated with fresh medium and images of wounds were taken under a phase contrast microscope at 0, 24, and 48 hours after wounding. The experiments were performed in triplicate.

Results

Identification of ADAMTS8 as a downregulated gene at 11q24.2-25

A deletion at 11q24.2-25 was frequently detected in a panel of NPC and ESCC tumor cell lines by 1-Mb aCGH (Fig. 1A). Expression profiling of all the 34 genes within this deletion was further analyzed by semiquantitative RT-PCR

Figure 1. *ADAMTS8* is a candidate TSG located at 11q25. A, schematic diagram showing the relative gene locus of *ADAMTS8* in 11q25 and the exon/intron structure of its transcript. The position of *ADAMTS8* in chromosome 11 is labeled according to Ensembl (<http://www.ensembl.org/>). The forward and reverse RT-PCR primers are indicated with arrows. Other genes located adjacent to the *ADAMTS8* locus are also shown. Structure of the predicted CGI spanning *ADAMTS8* promoter and exon 1. Each vertical line represents one CpG site. Respective positions of MSP and BGS primers, and the region analyzed by BGS are indicated by arrows. B, semiquantitative RT-PCR shows *ADAMTS8* is broadly expressed in normal adult tissues and fetal tissues except for bone marrow, with *GAPDH* as an internal control. Sk. M., skeletal muscle; B.M., bone marrow; L.N., lymph node.



(data not shown). *ADAMTS8* was found to be silenced in virtually all the NPC cell lines studied, but readily expressed in immortalized normal nasopharyngeal epithelial cell line and normal tissues of larynx and trachea as well as other normal adult and fetal tissues with varying expression levels except for bone marrow (Figs. 1B and 2A). In addition, frequent silencing or downregulation of *ADAMTS8* was also observed in multiple other carcinoma cell lines, including 6 of 6 NPC (100%), 12 of 16 ESCC (75%), 14 of 16 gastric (88%) and 4 of 5 CRC (80%), 11 of 13 HCC (85%), 3 of 5 Lung (60%), 7 of 9 breast (78%), 5 of 7 RCC (71%), and 3 of 4 cervical (75%) cancers (Fig. 2A and B and Supplementary Fig. S1 and Table S2). We further assessed *ADAMTS8* expression in representative nasopharyngeal, esophageal, and colon carcinoma cell lines by qPCR. As expected, we confirmed that *ADAMTS8* was frequently downregulated in tumor cell lines, but readily expressed in normal tissues, consistent with the semiquantitative RT-PCR results. These data suggest that *ADAMTS8* is a candidate tumor suppressor.

Promoter methylation of *ADAMTS8* contributes to its silencing

To investigate the mechanism of *ADAMTS8* downregulation in tumors, we first evaluated its genetic alterations. Multiplex differential genomic DNA-PCR for *ADAMTS8* and *APRT* was performed to detect *ADAMTS8* deletion in a region spanning exon 1 and exon 2. Results showed that homozygous or hemizygous deletion was detected in several tumor cell lines with or without silenced *ADAMTS8* (Sup-

plementary Fig. S2), suggesting that genetic alterations are one of the mechanisms for *ADAMTS8* silencing. Moreover, analysis of *ADAMTS8* mutations using online database (Wellcome Trust Cancer Genome Project, <http://www.sanger.ac.uk>) revealed only one missense somatic mutation of *ADAMTS8* reported in glioblastoma (29), indicating that its genetic sequence mutation is uncommon in tumors.

A typical CpG Island (CGI) spanning the exon 1 of *ADAMTS8* is predicted by CpG Island Searcher (<http://cpgislands.usc.edu/>; Fig. 1A). Thus, promoter methylation of *ADAMTS8* was further examined by MSP and found to be frequently detected in multiple carcinoma cell lines, including 100% of NPC, 44% of ESCC, 56% of gastric, 78% of CRC, 8% of HCC, 22% of breast, 43% of RCC, and 29% of cervical cancers (Fig. 2A and Supplementary Fig. S1 and Table S2), but seldom in lung cancer cell lines and not in normal epithelial cell lines (Fig. 2A). MSP results were further confirmed using high-resolution BGS of 63 CpG sites spanning the *ADAMTS8* CGI (Fig. 2B). We also noted that no methylation was detected in several cell lines with silenced or reduced *ADAMTS8*, including ESCC cell lines: EC1, EC18, HKESC1, HKESC2, KYSE140, KYSE180, KYSE510, and KYSE520 and gastric tumor cell lines: SNU16, YCC1, YCC7, and YCC16, indicating that other regulatory mechanisms such as histone modifications might also be involved.

We further found that *ADAMTS8* expression was restored after treatment with DNA methyltransferase inhibitor Aza, or in combination with TSA, accompanied by concomitant decrease of methylated alleles and

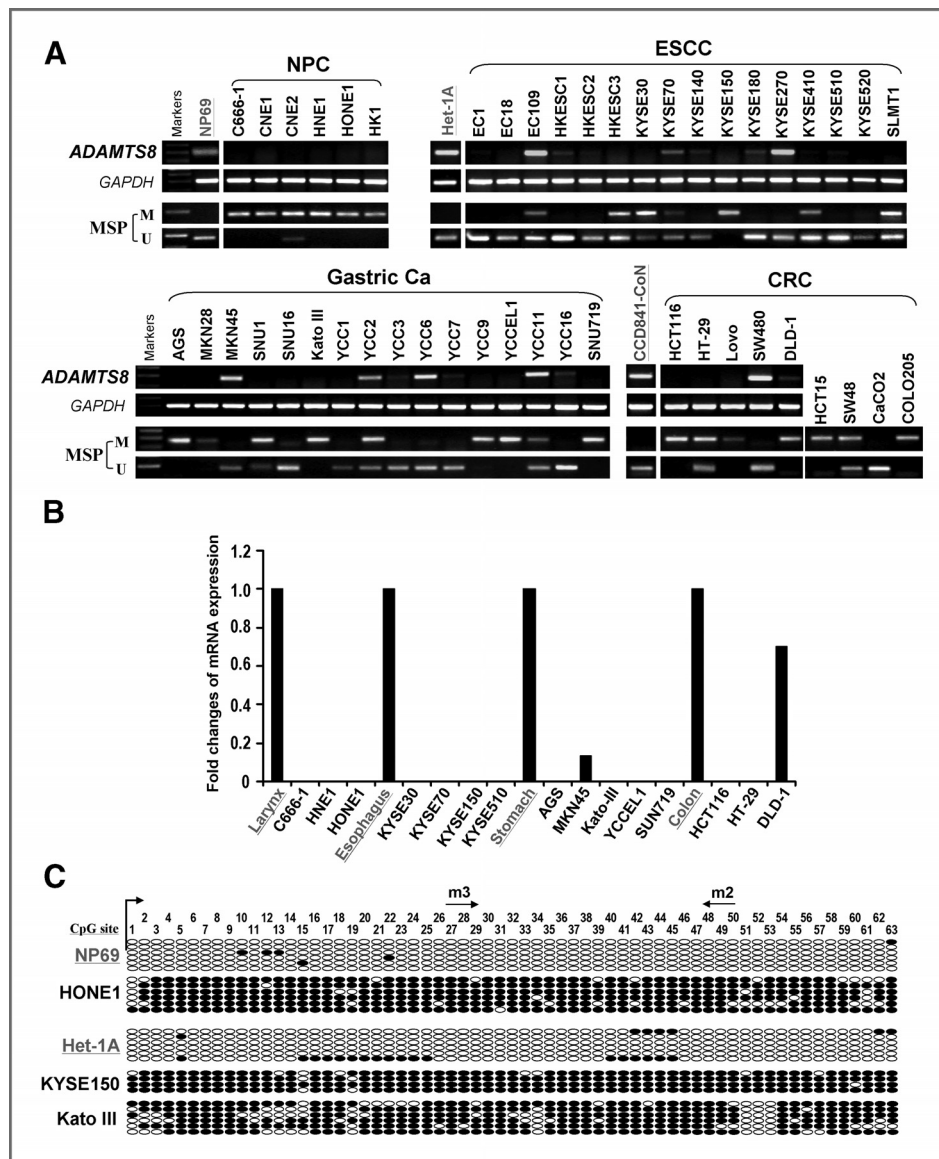


Figure 2. Epigenetic inactivation of *ADAMTS8* in multiple tumor cell lines. A, analyses of *ADAMTS8* expression and promoter methylation in tumor cell lines and normal controls. Immortalized normal epithelial cells are underlined. M, methylated; U, unmethylated; NPC, nasopharyngeal carcinoma; ESCC, esophageal squamous cell carcinoma; CRC, colorectal carcinoma; Ca, carcinoma. B, *ADAMTS8* expression was detected in representative tumor cell lines and normal tissues by quantitative RT-PCR. The expression level of each sample was normalized to internal control *GAPDH*. Fold change of *ADAMTS8* expression was calculated relative to that of normal tissue. C, representative BGS analyses of *ADAMTS8* promoter methylation in tumor cells and immortalized normal epithelial cells. The *ADAMTS8* transcription start site is indicated with a bent arrow. Circles, CpG sites analyzed; row of circles, an individual promoter allele that was cloned, randomly selected, and sequenced; filled circle, methylated CpG site; open circle, unmethylated CpG site.

increased unmethylated alleles in silenced tumor cells (Fig. 3A and C). Reactivation of *ADAMTS8* and complete demethylation were also observed in a genetic demethylation model using colorectal cell line (HCT116) with genetic double knockout of both DNA methyltransferase DNMT1 and DNMT3B (DKO; Fig. 3B and C). These results suggest that *ADAMTS8* is an epigenetic-regulated TSG, and promoter methylation is a major mechanism mediating *ADAMTS8* silencing in tumors.

Frequent *ADAMTS8* methylation detected in primary carcinomas

We next examined *ADAMTS8* methylation in primary tumors. *ADAMTS8* methylation was detected in 88% (36/41) of primary NPC, 58% (69/119) of gastric, 27% (3/11) of CRC, 22% (8/36) of ESCC, and 6% (3/47) of HCC tumor samples (Fig. 3E and Supplementary Table S2), but

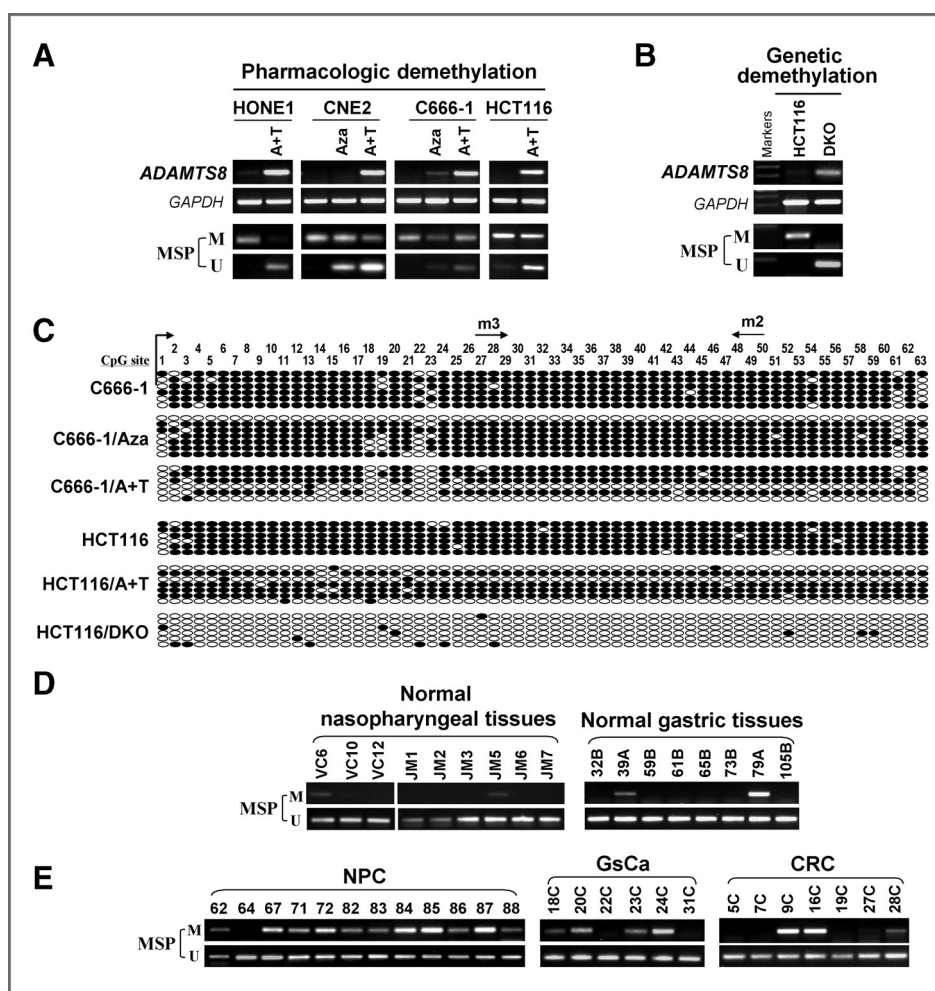
rarely observed in normal nasopharyngeal tissues (2/11, 18%), and normal gastric tissues (3/18, 17%; Fig. 3D and Supplementary Table S2). Thus, *ADAMTS8* methylation is frequent during tumor pathogenesis.

Although the frequency of *ADAMTS8* methylation in gastric cancer was high, further investigation on patients with gastric cancer showed no correlations between the *ADAMTS8* methylation status and clinical parameters including gender, *Helicobacter pylori* infection, TNM stage, Lauren type, and tumor differentiation (data not shown).

ADAMTS8 is a secreted protease inhibiting tumor cell clonogenicity by inducing apoptosis

ADAMTS8 is a secreted protease with a signal peptide at its N-terminus according to bioinformatics analysis (pTARGET, <http://bioapps.rit.albany.edu/>; Fig. 4A). We next

Figure 3. Reactivation of *ADAMTS8* by pharmacologic and genetic demethylation. A, restoration of *ADAMTS8* expression by pharmacologic demethylation using Aza (A) and TSA (T). B, genetic demethylation also activated *ADAMTS8* expression in HCT116 cell line with double knockout of DNMT1 and DNMT 3B (DKO). *ADAMTS8* mRNA level was measured by semiquantitative RT-PCR, and its methylation status was detected by MSP. C, detailed BGS analysis confirmed promoter demethylation of *ADAMTS8* with pharmacologic and genetic demethylation. The *ADAMTS8* transcription start site is indicated using a bent arrow. Circles, CpG sites analyzed; row of circles, an individual promoter allele that was cloned, randomly selected, and sequenced; filled circle, methylated CpG site; open circle, unmethylated CpG. D, E, representative analyses of *ADAMTS8* methylation in certain primary tumors and normal tissues by MSP. M, methylated; U, unmethylated; NPC, nasopharyngeal carcinoma; GsCa, gastric carcinoma; CRC, colorectal carcinoma.



selected NPC cell line HONE1 and ESCC cell line KYSE150 with silenced and methylated *ADAMTS8* as tumor model for following functional and mechanical studies. Subcellular localization of *ADAMTS8* by confocal microscopy showed that *ADAMTS8* was mainly localized to the cell membrane (Fig. 4B).

Culturing media from *ADAMTS8*-transfected KYSE150 cells and HONE1 cells were collected and subjected to TCA protein precipitation for the detection of *ADAMTS8* expression by Western blot analysis. *ADAMTS8* protein was detected in both the medium and cell lysates of the transfected KYSE150 cells, with much higher expression in the medium (Fig. 4C). We also examined *ADAMTS8* expression in the medium of *ADAMTS8*-transfected HONE1 cells collected at 24, 48, and 72 hours, which all showed good growth status as measured by cell-proliferation assay (Supplementary Fig. S3A). We found that *ADAMTS8* protein level was gradually decreased in a time-dependent manner, with no expression of α -tubulin detected, a marker of total cell lysate (Supplementary Fig. S3B). These results reveal that *ADAMTS8* could be secreted into the culturing media, thus as a secreted protease.

We further evaluated the impact of *ADAMTS8* expression on growth inhibition and apoptosis of tumor cells. Ectopic expression of *ADAMTS8* in HONE1 and KYSE150 cells resulted in significant reduction of colony numbers, compared with controls (Fig. 4D; $P < 0.05$). As reduction of tumor cell clonogenicity could be attributed to the induction of apoptosis (30), TUNEL assay was performed, increased TUNEL-positive cells were observed in *ADAMTS8* transfected-KYSE150 and HONE1 cells, together with increased apoptotic marker cleaved PARP (Fig. 4E). In addition, *ADAMTS8*-expressing HONE1 and KYSE150 cells underwent obvious cell shrinkage, DNA condensation, and fragmentation, which are distinct hallmarks of apoptosis (Supplementary Fig. S3C and S3D). These data demonstrate that *ADAMTS8* exerts tumor suppressive function through inducing apoptosis and inhibiting cell growth.

ADAMTS8 negatively modulates the EGFR–MEK–ERK signaling pathway

As metalloproteases have been shown involved in tumorigenesis through regulating EGFR signaling (31, 32), we investigated the impact of *ADAMTS8* on the EGFR signaling pathway. Culturing medium from KYSE150 cells

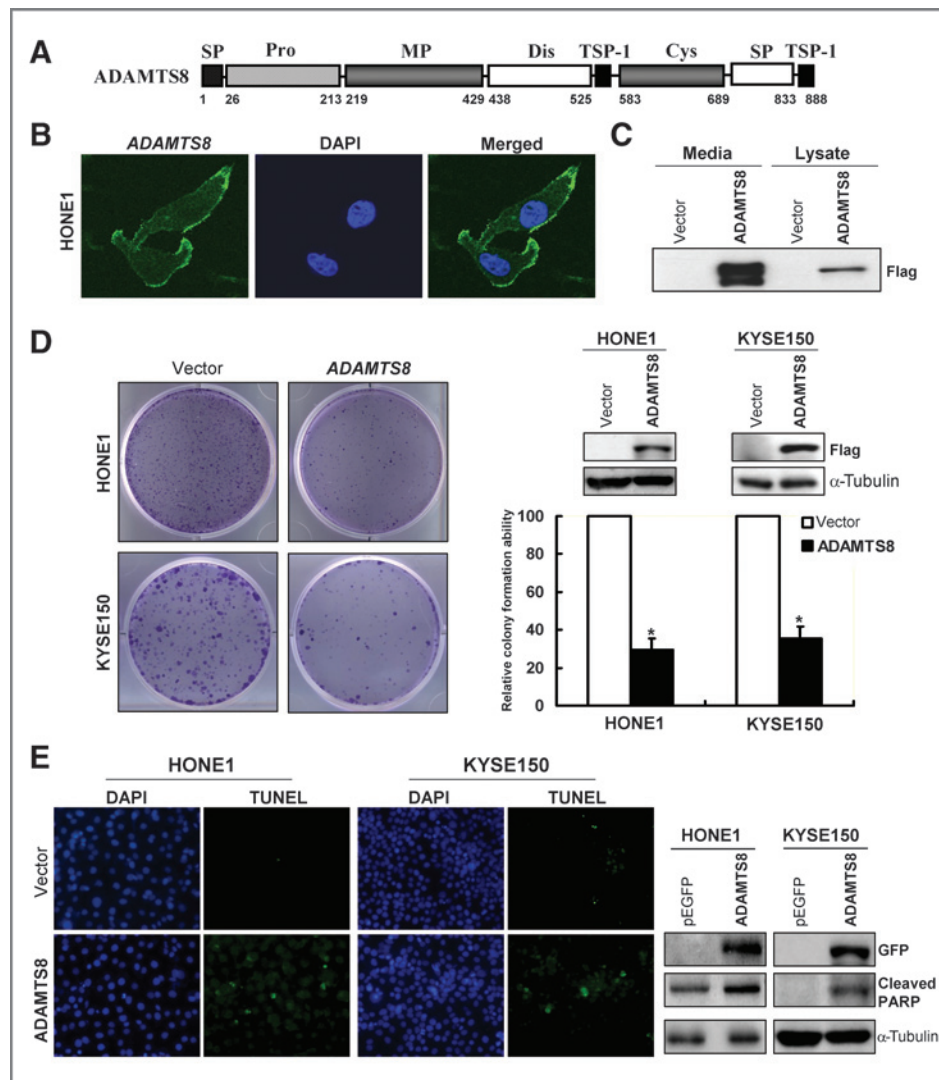


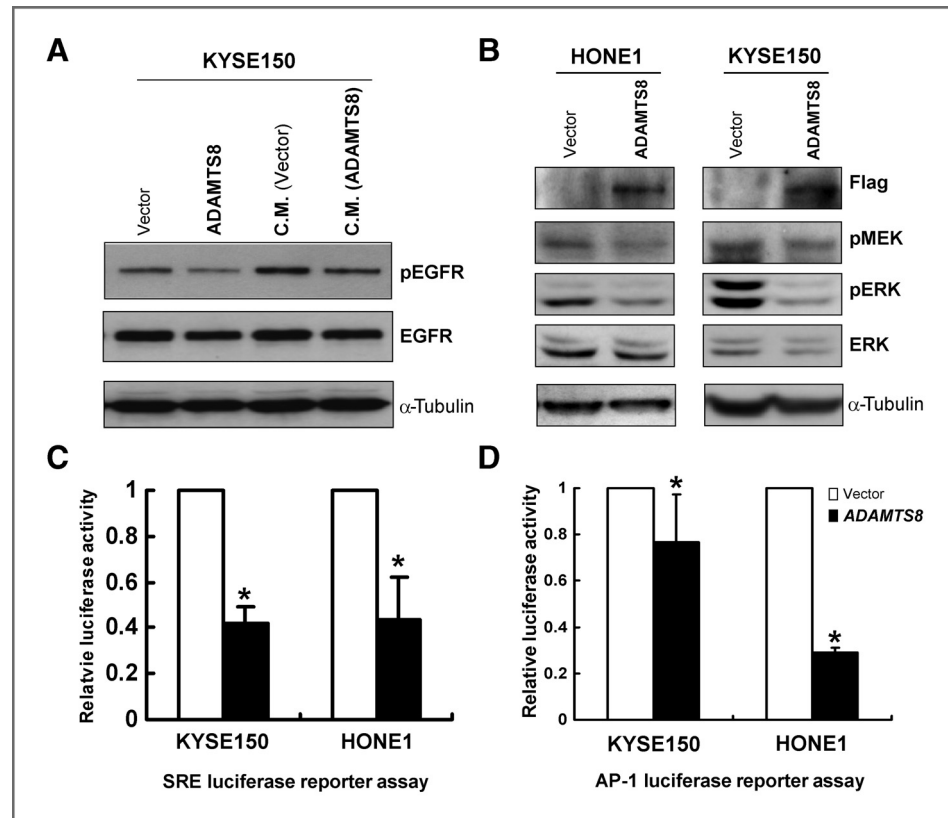
Figure 4. ADAMTS8 is a functional TSG that inhibits clonogenicity and induces apoptosis of tumor cells. **A**, protein structure of ADAMTS8 metalloprotease with different domains as illustrated: SS, signal sequence; Pro, prodomain; MP, metalloprotease domain; Dis, disintegrin domain; Cys, ADAM cysteine-rich domain; SP, spacer domain; and TSP-1, thrombospondin type 1 repeats. **B**, confocal microscopy assay showed that ADAMTS8 (green) was localized at cell membrane in ADAMTS8-transfected HONE1 cells. DAPI counterstaining (blue) was used to visualize DNA. Original magnification, $\times 400$. **C**, the detection of ADAMTS8 protein by Western blot analysis in both cell lysate and media. Culturing media were collected from ADAMTS8- or vector-transfected KYSE150 cells for 24 hours. Cell lysate was collected at 48 hours after transfection. **D**, representative colony formation assay with monolayer culture (left). Ectopic ADAMTS8 expression in tumor cells was confirmed by Western Blot analysis (right, upper). Quantitative analysis of colony formation ability in ADAMTS8-transfected cells (right, lower). The number of G418-resistant colonies in each vector-transfected cells was set as 100 (*, $P < 0.05$). **E**, the proapoptotic effect of ADAMTS8 in both HONE1 and KYSE150 cells was assessed by TUNEL assay (left). TUNEL-positive cells (green) are counted as apoptotic cells. Western blot analysis showing upregulation of cleaved PARP in ADAMTS8-transfected tumor cells (right).

transfected with ADAMTS8 was collected as conditioned medium, and conditioned medium from empty vector-transfected cells was used as control. We found decreased phosphorylation of EGFR in cells treated with KYSE150-transfected ADAMTS8 conditioned medium for 24 hours, with little change of total EGFR expression. Similar inhibitory effects were also observed in the total cell lysate from transfected cells (Fig. 5A).

We further examined the effects of ADAMTS8 expression on some downstream effectors of EGFR, such as MEK-ERK signaling. Results showed that ectopic expres-

sion of ADAMTS8 significantly reduced phosphorylation of MEK and ERK, with no effect on the total level of ERK (Fig. 5B). SRE and AP-1 luciferase reporter assays were further used to measure the modulation of MAPK signaling by ADAMTS8. In agreement with the inhibitory effect of ADAMTS8 on MEK and ERK phosphorylation, transcriptional activities of SRE and AP-1 reporters were significantly decreased in ADAMTS8-expressing HONE1 and KYSE150 cells ($P < 0.05$; Fig. 5C and D). These data indicate that ADAMTS8 indeed negatively regulates EGFR–MEK–ERK signaling.

Figure 5. Secreted ADAMTS8 inhibits EGFR–MEK–ERK signaling. A, Western blot analysis of phosphorylated EGFR and total EGFR in both *ADAMTS8*-expressing KYSE150 cell lysate and cells treated with CM containing ADAMTS8 for 24 hours. B, phosphorylated MEK, ERK, and total ERK as measured by Western blot analysis in *ADAMTS8* or vector-transfected HONE1 and KYSE150 cells. C, D, SRE and AP-1 luciferase reporter activity assays in vector- and *ADAMTS8*-expressing tumor cells. Cells were cotransfected with either vector or *ADAMTS8*, together with pSRE-Luc or pAP-1 reporter plasmids and renilla reporter plasmid. The activity of luciferase was normalized with the renilla activity. Data shown are means \pm SE of triplicate transfections in 3 independent experiments. Asterisk indicates statistically significant difference (*, $P < 0.05$).



ADAMTS8 suppresses cell migration by disrupting stress fiber formation

As EGFR–MEK–ERK signaling activation is implicated in actin cytoskeletal reorganization and cell migration, the role of ADAMTS8 on actin filament integrity and tumor cell motility was further investigated. Results showed that actin stress fibers were disassembled in *ADAMTS8*-expressing HONE1 cells, but not in control cells (Fig. 6A). Cell motility of ADAMTS8-transfected KYSE150 cells displayed a marked delay in wound closure compared with controls, as measured by wound-healing assay (Fig. 6B), suggesting that ADAMTS8 inhibits migration of tumor cells via disrupting stress filament integrity.

Discussion

In this work, we found that *ADAMTS8* is frequently silenced in multiple carcinoma cell lines but broadly expressed in human normal adult and fetal tissues. Promoter methylation seems to be a major mechanism inactivating *ADAMTS8*, although genetic alterations or histone modifications may also be involved. We also found that ADAMTS8 functions as a proapoptotic tumor suppressor through antagonizing EGFR–MEK–ERK signaling, further suppresses tumor cells migration through disrupting stress fiber formation (Fig. 6C).

Although as demonstrated here and in other studies, *ADAMTS8* is downregulated in multiple cancers, few studies have reported about its function and related mechanism

in tumorigenesis. Our study seems to be the first to reveal that ADAMTS8 possesses antitumor properties and its underlying mechanism besides previously reported role in anti-angiogenesis. We found that ADAMTS8 metalloprotease exerts tumor suppressive functions by inhibiting tumor cell clonogenicity, eliciting apoptosis, and restraining tumor cell migration. As apoptotic property has not been reported for ADAMTS members, this study indicates the possibility that other ADAMTS members may also involve in the regulation of apoptosis. We further found that the inhibition of tumor cell growth and induction of apoptosis by ADAMTS8 are associated with deregulation of EGFR–MEK–ERK signaling pathway, and secreted ADAMTS8 also exhibits inhibitory effect on EGFR signaling, in line with the findings in ADAMTS1 and ADAMTS15, another 2 members of the same subgroup (4, 33). Thus, we report here that ADAMTS8 is another ADAMTS member displaying antitumorigenic (4, 33, 34).

It is intriguing that ADAM and ADAMTS members are often observed to possess opposing roles in tumorigenesis and the modulation of EGFR–ERK signaling, although they both belong to the metzincin-superfamily of Zinc-dependent metalloproteinases (35). Proteolytic function of ADAMTS8 as an aggrecanase was demonstrated previously (36). The TSP-1 domain present in ADAMTS members but absent in ADAM group is responsible for this opposite behavior (7). Ectopic expression of TSP-1 was shown to block MAPK signaling activation and slow down tumor formation (37), whereas cells with mutated form of

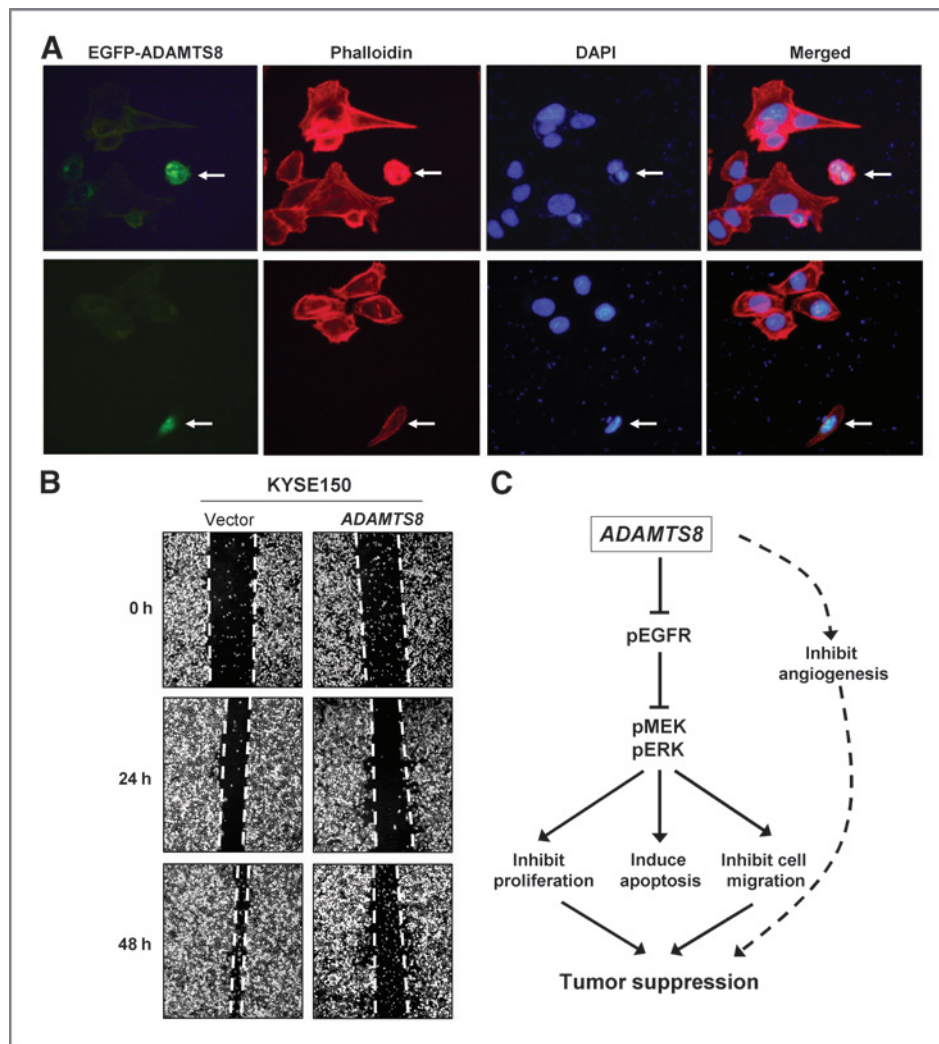


Figure 6. Ectopic expression of ADAMTS8 inhibits cancer cell migration. A, phalloidin staining of cells shows that expression of ADAMTS8 disrupts actin stress fiber formation. B, effect of ADAMTS8 on cell migration was assessed by wound-healing motility assay. Confluent monolayers of vector- and ADAMTS8-transfected KYSE150 tumor cells were scratched 48 hours after transfection. Phase-contrast microscopy photos of wound margins were taken at 24 and 48 hours after scratching. C, proposed mechanism of the tumor suppressive function of ADAMTS8 through suppressing the EGFR–MEK–ERK signaling pathway.

ADAMTS15 lacking 2 TSP-1 motifs had elevated ERK phosphorylation level compared with cells harboring wild-type ADAMTS15 (4). In addition, TSP-1 in auto-proteolytic cleaved ADAMTS1 is required for inhibiting ERK (2). Therefore, the TSP-1 domain in ADAMTS members is likely involved in suppressing the activated MEK–ERK signaling in cancer cells.

Most metalloproteinases are regarded as key regulators of tumor cell invasiveness, because they possess proteolytic activities to destruct the ECM and alter the cell–cell attachments and cell–matrix attachments, which are integral to tumor cell migration (38). However, little is known about the involvement of ADAMTS members in cell invasion except for ADAMTS1 and ADAMTS5. Full-length ADAMTS1 and ADAMTS5 are reported to promote metastasis whereas fragment of ADAMTS1 was shown to be antimetastatic (2, 39). Here, we also identified that ADAMTS8 suppressed tumor cell migration by disrupting actin polymerization. Further study of ADAMTS8 on cell epithelial–mesenchymal transition is needed.

In summary, our study shows that ADAMTS8 functions as a proapoptotic TSG through suppressing EGFR–MEK–ERK signaling, which is frequently silenced by promoter CpG methylation in common carcinomas. However, further investigations are needed to show exact feature and function of ADAMTS8 in connection to cellular homeostasis.

Disclosure of Potential Conflicts of Interest

No potential conflicts of interest were disclosed.

Authors' Contributions

Conception and design: G.C.G. Choi, Q. Tao

Development of methodology: G.C.G. Choi, S.W. Tsao, Q. Tao

Acquisition of data (provided animals, acquired and managed patients, provided facilities, etc.): G.C.G. Choi, J. Li, Y. Wang, L. Li, X. Su, T. Xiang, S.Y. Rha, Q. Tao

Analysis and interpretation of data (e.g., statistical analysis, biostatistics, computational analysis): G.C.G. Choi, J. Li, Y. Wang, L. Li, L. Zhong, Q. Tao

Writing, review, and/or revision of the manuscript: G.C.G. Choi, Y. Wang, L. Li, S.Y. Rha, A.T.C. Chan, Q. Tao

Administrative, technical, or material support (i.e., reporting or organizing data, constructing databases): L. Li, X. Su, J. Ying, J. Yu, A.T.C. Chan, Q. Tao

Study supervision: B. Ma, J.J.Y. Sung, A.T.C. Chan, Q. Tao

Acknowledgments

The authors thank Dr. B. Vogelstein for HCT116 cells with knockout of DNMTs, and DSMZ (German Collection of Microorganisms & Cell Cultures) for the KYSE cell lines (Shimada et al., 1992).

Grant Support

This study was supported by grants from Hong Kong RGC (GRF #475009), National Natural Science Foundation (#81172582 and

#81201934), and the Group Research Schemes of The Chinese University of Hong Kong.

The costs of publication of this article were defrayed in part by the payment of page charges. This article must therefore be hereby marked *advertisement* in accordance with 18 U.S.C. Section 1734 solely to indicate this fact.

Received April 22, 2013; revised September 17, 2013; accepted September 30, 2013; published OnlineFirst November 1, 2013.

References

- Lopez-Otin C, Matrisian LM. Emerging roles of proteases in tumour suppression. *Nat Rev Cancer* 2007;7:800–8.
- Liu YJ, Xu Y, Yu Q. Full-length ADAMTS-1 and the ADAMTS-1 fragments display pro- and antimetastatic activity, respectively. *Oncogene* 2006;25:2452–67.
- Moncada-Pazos A, Obaya AJ, Fraga MF, Viloria CG, Capellá G, Gausachs M, et al. The ADAMTS12 metalloprotease gene is epigenetically silenced in tumor cells and transcriptionally activated in the stroma during progression of colon cancer. *J Cell Sci* 2009;122(Pt 16):2906–13.
- Viloria CG, Obaya AJ, Moncada-Pazos A, Llamazares M, Astudillo A, Capellá G, et al. Genetic inactivation of ADAMTS15 metalloprotease in human colorectal cancer. *Cancer Res* 2009;69:4926–34.
- Lo PH, Lung HL, Cheung AK, Apte SS, Chan KW, Kwong FM, et al. Extracellular protease ADAMTS9 suppresses esophageal and nasopharyngeal carcinoma tumor formation by inhibiting angiogenesis. *Cancer Res* 2010;70:5567–76.
- Jin H, Wang X, Ying J, Wong AH, Li H, Lee KY, et al. Epigenetic identification of ADAMTS18 as a novel 16q23.1 tumor suppressor frequently silenced in esophageal, nasopharyngeal and multiple other carcinomas. *Oncogene* 2007;26:7490–8.
- Tang BL. ADAMTS: a novel family of extracellular matrix proteases. *Int J Biochem Cell Biol* 2001;33:33–44.
- Rocks N, Paulissen G, El Hour M, Quesada F, Crahay C, Gueders M, et al. Emerging roles of ADAM and ADAMTS metalloproteinases in cancer. *Biochimie* 2008;90:369–79.
- Porter S, Scott SD, Sassoon EM, Williams MR, Jones JL, Girling AC, et al. Dysregulated expression of adamalysin-thrombospondin genes in human breast carcinoma. *Clin Cancer Res* 2004;10:2429–40.
- Llamazares M, Cal S, Quesada V, Lopez-Otin C. Identification and characterization of ADAMTS-20 defines a novel subfamily of metalloproteinases-disintegrins with multiple thrombospondin-1 repeats and a unique GON domain. *J Biol Chem* 2003;278:13382–9.
- Cauwe B, Van den Steen PE, Opdenakker G. The biochemical, biological, and pathological kaleidoscope of cell surface substrates processed by matrix metalloproteinases. *Crit Rev Biochem Mol Biol* 2007;42:113–85.
- Vazquez F, Hastings G, Ortega MA, Lane TF, Oikemus S, Lombardo M, et al. METH-1, a human ortholog of ADAMTS-1, and METH-2 are members of a new family of proteins with angio-inhibitory activity. *J Biol Chem* 1999;274:23349–57.
- Koo BH, Coe DM, Dixon LJ, Somerville RP, Nelson CM, Wang LW, et al. ADAMTS9 is a cell-autonomously acting, anti-angiogenic metalloprotease expressed by microvascular endothelial cells. *Am J Pathol* 2010;176:1494–504.
- Dunn JR, Reed JE, du Plessis DG, Shaw EJ, Reeves P, Gee AL, et al. Expression of ADAMTS-8, a secreted protease with antiangiogenic properties, is downregulated in brain tumours. *Br J Cancer* 2006;94:1186–93.
- Dunn JR, Panutsopoulos D, Shaw MW, Heighway J, Dormer R, Salmo EN, et al. METH-2 silencing and promoter hypermethylation in NSCLC. *Br J Cancer* 2004;91:1149–54.
- Demircan K, Gunduz E, Gunduz M, Beder LB, Hirohata S, Nagatsuka H, et al. Increased mRNA expression of ADAMTS metalloproteinases in metastatic foci of head and neck cancer. *Head Neck* 2009;31:793–801.
- Masui T, Hosotani R, Tsuji S, Miyamoto Y, Yasuda S, Ida J, et al. Expression of METH-1 and METH-2 in pancreatic cancer. *Clin Cancer Res* 2001;7:3437–43.
- Rodríguez-Rodero S, Fernandez AF, Fernandez-Morera JL, Castro-Santos P, Bayon GF, Ferrero C, et al. DNA methylation signatures identify biologically distinct thyroid cancer subtypes. *J Clin Endocrinol Metab* 2013;98:2811–21.
- Cheng Y, Geng H, Cheng SH, Liang P, Bai Y, Li J, et al. KRAB zinc finger protein ZNF382 is a proapoptotic tumor suppressor that represses multiple oncogenes and is commonly silenced in multiple carcinomas. *Cancer Res* 2010;70:6516–26.
- Li L, Ying J, Li H, Zhang Y, Shu X, Fan Y, et al. The human cadherin 11 is a pro-apoptotic tumor suppressor modulating cell stemness through Wnt/ β -catenin signaling and silenced in common carcinomas. *Oncogene* 2012;31:3901–12.
- Ying J, Li H, Seng TJ, Langford C, Srivastava G, Tsao SW, et al. Functional epigenetics identifies a protocadherin PCDH10 as a candidate tumor suppressor for nasopharyngeal, esophageal and multiple other carcinomas with frequent methylation. *Oncogene* 2006;25:1070–80.
- Tao Q, Huang H, Geiman TM, Lim CY, Fu L, Qiu GH, et al. Defective *de novo* methylation of viral and cellular DNA sequences in ICF syndrome cells. *Hum Mol Genet* 2002;11:2091–102.
- Qiu GH, Tan LK, Loh KS, Lim CY, Srivastava G, Tsai ST, et al. The candidate tumor suppressor gene BLU, located at the commonly deleted region 3p21.3, is an E2F-regulated, stress-responsive gene and inactivated by both epigenetic and genetic mechanisms in nasopharyngeal carcinoma. *Oncogene* 2004;23:4793–806.
- Li L, Tao Q, Jin H, van Hasselt A, Poon FF, Wang X, et al. The tumor suppressor UCHL1 forms a complex with p53/MDM2/ARF to promote p53 signaling and is frequently silenced in nasopharyngeal carcinoma. *Clin Cancer Res* 2010;16:2949–58.
- Xu L, Li X, Chu ES, Zhao G, Go MY, Tao Q, et al. Epigenetic inactivation of BCL6B, a novel functional tumour suppressor for gastric cancer, is associated with poor survival. *Gut* 2011;61:977–85.
- Shu XS, Li L, Ji M, Cheng Y, Ying J, Fan Y, et al. FEZF2, a novel 3p14 tumor suppressor gene, represses oncogene EZH2 and MDM2 expression and is frequently methylated in nasopharyngeal carcinoma. *Carcinogenesis* 2013;34:1984–93.
- Tao Q, Swinnen LJ, Yang J, Srivastava G, Robertson KD, Ambinder RF. Methylation status of the Epstein-Barr virus major latent promoter C in iatrogenic B cell lymphoproliferative disease. Application of PCR-based analysis. *Am J Pathol* 1999;155:619–25.
- Ying J, Li H, Yu J, Ng KM, Poon FF, Wong SC, et al. WNT5A exhibits tumor-suppressive activity through antagonizing the Wnt/ β -catenin signaling, and is frequently methylated in colorectal cancer. *Clin Cancer Res* 2008;14:55–61.
- Parsons DW, Jones S, Zhang X, Lin JC, Leary RJ, Angenendt P, et al. An integrated genomic analysis of human glioblastoma multiforme. *Science* 2008;321:1807–12.
- Ballif BA, Blenis J. Molecular mechanisms mediating mammalian mitogen-activated protein kinase (MAPK) kinase (MEK)-MAPK cell survival signals. *Cell Growth Differ* 2001;12:397–408.
- Marcoux N, Vuori K. EGF receptor activity is essential for adhesion-induced stress fiber formation and cofilin phosphorylation. *Cell Signal* 2005;17:1449–55.
- Toral C, Solano-Agama C, Reyes-Marquez B, Sabanero M, Talamás P, González del Pliego M, et al. Role of extracellular matrix-cell interaction

- and epidermal growth factor (EGF) on EGF-receptors and actin cytoskeleton arrangement in infantile pituitary cells. *Cell Tissue Res* 2007;327:143–53.
33. Suga A, Hikasa H, Taira M. Xenopus ADAMTS1 negatively modulates FGF signaling independent of its metalloprotease activity. *Dev Biol* 2006;295:26–39.
 34. Llamazares M, Obaya AJ, Moncada-Pazos A, Heljasvaara R, Espada J, López-Otín C, et al. The ADAMTS12 metalloproteinase exhibits anti-tumorigenic properties through modulation of the Ras-dependent ERK signalling pathway. *J Cell Sci* 2007;120(Pt 20):3544–52.
 35. Duffy MJ, McKiernan E, O'Donovan N, McGowan PM. Role of ADAMs in cancer formation and progression. *Clin Cancer Res* 2009;15:1140–4.
 36. Collins-Racie LA, Flannery CR, Zeng W, Corcoran C, Annis-Freeman B, Agostino MJ, et al. ADAMTS-8 exhibits aggrecanase activity and is expressed in human articular cartilage. *Matrix Biol* 2004;23:219–30.
 37. Zhang YW, Su Y, Volpert OV, Vande Woude GF. Hepatocyte growth factor/scatter factor mediates angiogenesis through positive VEGF and negative thrombospondin 1 regulation. *Proc Natl Acad Sci U S A* 2003;100:12718–23.
 38. Yoon SO, Park SJ, Yun CH, Chung AS. Roles of matrix metalloproteinases in tumor metastasis and angiogenesis. *J Biochem Mol Biol* 2003;36:128–37.
 39. Nakada M, Miyamori H, Kita D, Takahashi T, Yamashita J, Sato H, et al. Human glioblastomas overexpress ADAMTS-5 that degrades brevican. *Acta Neuropathol* 2005;110:239–46.

Molecular Cancer Research

The Metalloprotease ADAMTS8 Displays Antitumor Properties through Antagonizing EGFR–MEK–ERK Signaling and Is Silenced in Carcinomas by CpG Methylation

Gigi C.G. Choi, Jisheng Li, Yajun Wang, et al.

Mol Cancer Res 2014;12:228-238. Published OnlineFirst November 1, 2013.

Updated version Access the most recent version of this article at:
doi:[10.1158/1541-7786.MCR-13-0195](https://doi.org/10.1158/1541-7786.MCR-13-0195)

Cited articles This article cites 39 articles, 17 of which you can access for free at:
<http://mcr.aacrjournals.org/content/12/2/228.full.html#ref-list-1>

E-mail alerts [Sign up to receive free email-alerts](#) related to this article or journal.

Reprints and Subscriptions To order reprints of this article or to subscribe to the journal, contact the AACR Publications Department at pubs@aacr.org.

Permissions To request permission to re-use all or part of this article, contact the AACR Publications Department at permissions@aacr.org.